

See discussions, stats, and author profiles for this publication at: <https://www.researchgate.net/publication/24175323>

Fabry-Pérot optical filter assembly: a candidate for the Mie/ Rayleigh separator in EarthCARE

Article in *Optics Express* · February 2009

DOI: 10.1364/OE.17.003476 · Source: PubMed

CITATIONS

8

READS

506

10 authors, including:



Michael Foster

IS Instruments Ltd

55 PUBLICATIONS 1,009 CITATIONS

SEE PROFILE



Jonathan Storey

IS-Instruments Ltd.

19 PUBLICATIONS 141 CITATIONS

SEE PROFILE



Carl Thwaite

ABSL Space Products

11 PUBLICATIONS 61 CITATIONS

SEE PROFILE



Ivelin Bakalski

Sigma Space (division of Hexagon US Federal)

16 PUBLICATIONS 70 CITATIONS

SEE PROFILE

Fabry-Pérot optical filter assembly: a candidate for the Mie/ Rayleigh separator in EarthCARE

M.J. Foster,^{1*} R. Bond,² J. Storey,¹ C. Thwaite,² J.Y. Labandibar,³ I. Bakalski,¹ A. Hélière,⁴ A. Delev,¹ D. Rees,¹ and M. Slimm²

¹Lidar Technologies, Units 14-15 Tannery Road Industrial Estate, Tonbridge, Kent, TN9 1RF, UK,

²ABSL Space Products, Culham Science Centre, Abingdon, OXON, OX14 3ED, UK,

³Thales Alenia Space, Etablissement de Cannes, 100, Boulevard du Midi, BP 99, 06156, Cannes La Bocca Cedex, France,

⁴European Space Research and Technology Centre, Postbus 299, 2200 AG Noordwijk, The Netherlands,

* Corresponding Author: mfooster@hovemere.com

Abstract: This paper describes the development, characterisation and environmental testing of a high performance state-of-the-art optical filter for separating the Mie and Rayleigh backscatter signals for the ATLID LIDAR of the EarthCARE mission. The filter assembly utilises capacitance stabilised Fabry-Pérot étalon technology to provide high resolution optical filtering of the LIDAR signal, efficiently separating the two critical backscatter components from the atmosphere. The paper describes the development of the filter assembly and its subsequent performance testing. The filter has demonstrated state-of-the-art optical performance. Additionally, one of the étalons has been taken through complete environmental testing for space applications.

© 2009 Optical Society of America

OCIS codes: (120.0120) Instrumentation measurement and metrology; (120.2230) Fabry Pérot; (120.2440) Filters; (120.6085) Space instrumentation

References and links

1. EarthCARE: Earth Clouds Aerosol and Radiation Explorer Mission report ESA SP – 1279 (1) April (2004).
2. D. Rees, I. McWhirter, P. B. Hayes, and T. Dines, "A Stable, Rugged Capacitance-stabilized Piezo-electric Scanned Fabry-Pérot Etalon," **14**, J. Phys. E: Sci. Instrum. 11320-1325 (1981).
3. R. A. Bond, M. Foster, V. K. Thompson, D. Rees, and J. Pereira Do Carmo, "High Resolution Optical Filtering Technology," *22nd Int. Laser Radar Conf. (ILRC 2004)*, Metera, Italy, 12-16 July, (2004).
4. G. Hernandez, *Fabry-Pérot Interferometers* Cambridge (Cambridge University Press. ISBN 0521322383 1986).
5. D. Rees, T. J. Fuller-Rowell, A. Lyons, T. L. Killeen, and P. B. Hays, "Stable and Rugged Etalon for the Dynamics Explorer Fabry-Pérot Interferometer: I. Design and Construction," **21**, Appl. Opt. 3896-3902 (1982).
6. R.A. Hoffman, "Dynamics Explorer Program," *Eos61* (1980).

1. Introduction

Climate and a deep understanding of the meteorology of the Earth's atmosphere are two of the critical issues facing mankind today. The sixth Earth Explorer Mission [1], known as EarthCARE, is a joint Japanese/ European programme which aims to improve our understanding of the Earth's atmospheric systems. The current proposed launch date is 2013. The primary aim of the EarthCARE mission is to improve understanding of the radiative balance of the Earth's atmosphere and its description within climate and numerical weather forecast models.

One of the principle objectives of EarthCARE is to make profiled measurements of aerosols and clouds within the atmosphere. These measurements will be made partly by the European ATmospheric backscatter LIDar (ATLID) provided by ESA, and by a sophisticated

radar provided by JAXA for EarthCARE. The LIDAR will operate at 355 nm where the Rayleigh scattering cross section by molecules is high. A key requirement of the ATLID LIDAR is the separation of the Mie (aerosol) and Rayleigh (molecular) signatures, and the suppression of the high background signal from the sunlit atmosphere during daytime. This will allow the LIDAR observations of the aerosol and molecular signals to be analysed in detail.

This paper describes the development and space qualification of a high performance optical filter system capable of performing the separation of the Mie and Rayleigh backscattered signals applicable for EarthCARE. For example, the Mie channel filter must provide a spectral bandwidth of < 1 pm, with as high a transmission as possible, while suppressing the high level of background light present on the dayside due to scattered sunlight. Although the filter described here is targeted at EarthCARE, it clearly has wider application to all LIDAR instruments requiring optical filtering with high spectral resolution.

1.1 The Capacitance Stabilised Etalon

At the heart of the Atmospheric LIDAR Filter Assembly (ALFA) are two state-of-the-art high performance Fabry-Pérot étalon filters. Fabry-Pérot étalons have played a key role in the development in both space-borne and ground-based LIDAR instruments [2] providing both narrow band filtering and high transmission over a large optical aperture (i.e. high etendue) [3]. A comprehensive description of the properties of Fabry-Pérot étalons can be found in reference [4]. There are many different designs of Fabry-Pérot étalon. This development exploits the Capacitance-Stabilised Etalon (CSE) [1]. In optical performance terms, the CSE arguably represents the state-of-the-art in Fabry-Pérot technology [3].

A CSE utilises the combination of piezoelectric transducer elements to adjust the separation and parallelism of the étalon plates, with capacitor elements, in appropriate servo-loop circuits, to provide precise monitoring of the transducers. This enables both the plate parallelism and the plate separation to be precisely controlled [2], a capability that is not present in other Fabry-Pérot étalon designs. The CSE implements servo-loop feedback control of the plate position using a capacitance-bridge technique. This ensures precise control of the étalon at all times, and the étalon plate parallelism and Optical Path Difference can be adjusted on time-constants of less than 50 ms. So-called “Drive” capacitors act as proxy for the étalon Optical Path Difference (OPD), while “Reference” capacitors are used to monitor environmental changes.

The extensive development of the CSE technology for space applications is described in more detail in [2,4].

2. Filter requirements

The development of ALFA had two key objectives. The first was to produce a complete filter assembly which would meet the demanding optical and functional performance requirements of the filter sub-system for the ATLID/EarthCARE LIDAR instrument. The second objective was to demonstrate that the CSE met the engineering level environmental specifications, while verifying its optical performance after surviving vibration and thermal-vacuum testing.

The EarthCARE LIDAR generates three signal components of critical importance within the troposphere and low stratosphere from molecular and aerosol backscatter. ALFA must separate the Rayleigh, Mie Co-polar and Mie Cross-polar components of the atmospheric signal back-scattered to the EarthCARE LIDAR. A description of the geo physical information contained within the Mie and Rayleigh signal can be found within [1].

The FWHM and transmission targets for each of the three channels are:

Mie Co-polar	FWHM = 0.22 pm	Transmission = 45 %
Mie Cross-polar	FWHM = 12pm	Transmission = 55 %
Rayleigh	FWHM = 12 pm	Transmission = 50 %

In addition the BFA assembly (CSE and Interference filter combination) must suppress the background light such that $> 50\%$ of the light observed from the daytime sky is within the 12 pm FWHM of the BFA.

3. Design and development of the ALFA filter assembly

3.1 The Optical Configuration

Figure 1 shows, schematically, the overall layout of the Atmospheric LIDAR Filter Assembly (ALFA). The ALFA consists of two CSEs, one Interference Filter (IF), one Polarising Beam Splitter (PSA) and a $\frac{1}{4}$ Wave Plate.

The system has three channels, as follows:

- Channel 1: Rayleigh Channel
- Channel 2a: Mie Co-polar Channel
- Channel 2b: Mie Cross-polar Channel

The ALFA filter assembly works as follows: Light is directed into the system via a reflecting mirror and enters the Blocking Filter Assembly (BFA). The BFA consists of a narrow band Interference Filter and the first CSE. The BFA ensures the broad-band suppression of the background light whilst transmitting the Mie and Rayleigh components. After transmission through the BFA the signal passes through the Polarizing Beam Splitter (PBS) where the co-polar components are reflected and the cross-polar component is transmitted (forming the Mie cross-polar channel). The reflected component passes through the $\frac{1}{4}$ Wave Plate and enters the Medium Resolution Filter (MRF) where the second CSE transmits the narrow Mie component, while reflecting the light outside this narrow transmission band. By virtue of the double pass through the $\frac{1}{4}$ Wave Plate this light is then transmitted through the PBS, forming the Rayleigh channel.

Separating the Mie elements into co- and cross-polar components (with respect to the outgoing laser light) provides additional information regarding the nature of the aerosols producing the Mie scattering.

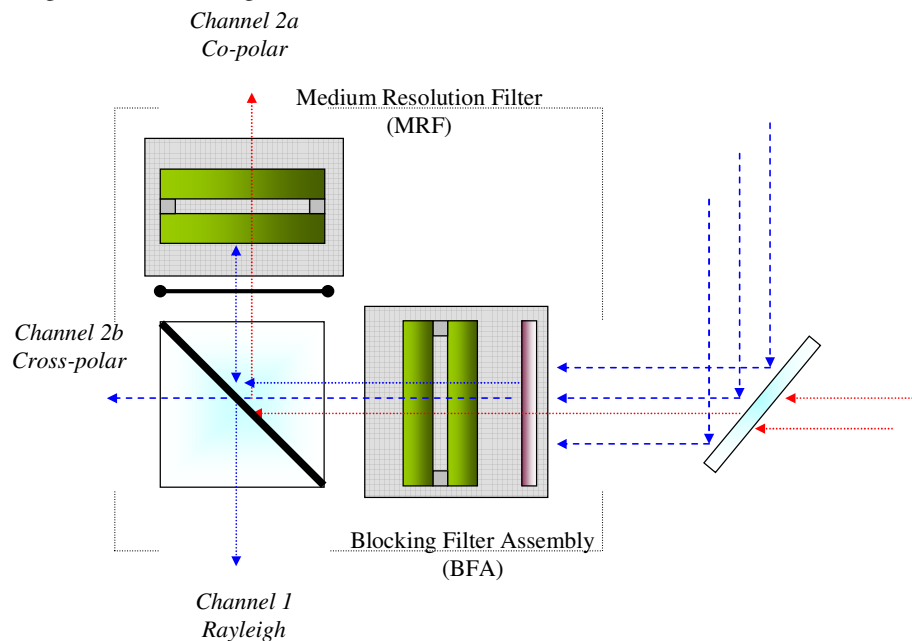


Fig. 1. Schematic diagram of the ALFA filter assembly.

For the purposes of all optical tests, the laser light is focused into an optical fibre before being collimated and transmitted into the ALFA assembly. This ensures that the light is unpolarised and thus the separation of the two polarisation planes can be measured accurately.

The key specifications for the BFA and MRF CSEs are given in Table 1. The interference Filter had a spectral bandwidth of 0.8 nm and a peak transmission of 79%. The divergence of the beam passing through the ALFA system is 0.5 mrad.

Table 1. Specifications for the BFA and MRF CSEs.

	BFA CSE	MRF CSE
Working aperture	38 mm	38 mm
OPD	140 μm	15 mm
FSR	0.45 nm	4.2 pm
Bandwidth (FWHM)	12 \pm 1 pm	0.22 \pm 0.1 pm
Overall finesse	34	19
Reflectivity	93 %	87 %
Tuning Range	> 2 FSR	> 2 FSR
Transmission	As high as possible	As high as possible

Whilst the bandwidth of the MRF CSE is much smaller than that of the BFA CSE, the different free-spectral ranges require that the BFA CSE has the larger finesse and thus it was the more challenging étalon to produce. The étalon finesse is directly linked to the transmission of the étalon as described by Eq. 1.

$$T = \frac{F_R}{F} \quad (1)$$

where F is the étalon's overall finesse and F_R is the reflective finesse of the étalon. The overall finesse is dependent on several contributions each of which depends on a particular characteristic of the étalon plates and optical configuration. The overall finesse is expressed approximately by the following equation:

$$\frac{1}{F^2} \approx \frac{1}{F_D^2} + \frac{1}{F_R^2} + \frac{1}{F_A^2} \quad (2)$$

where F_D is the defect finesse, F_R is the reflective finesse and F_A is the aperture finesse. The defect finesse is a function of the matching plate flatness. From the optimisation process the reflectivities of the BFA and MRF étalons were specified as 93 % and 87 % respectively. Since the targeted transmission for each of the étalons is 80 %, the plate flatness must be higher than $\lambda/200$ (at 633 nm) given the overall finesse and reflectivity values (Table 1).

The CSEs have a working aperture of 38 mm and specified OPDs of 140 μm and 15 mm. These define their usable FOV (Jacquinot criterion). The étalons do not have a specific design angle. For the purposes of the tests, the divergence of the beam of 0.5 mrad. (i.e. consistent with the Jacquinot criterion for such étalons used at 355 nm).

Both Fabry-Pérot étalons have an outside diameter of 72 mm, in order to accommodate the spacer and capacitor elements. Although the working aperture is 38 mm, the coated area is designed to be 42 mm, since this increases the probability of achieving the high value of defect finesse that is essential. With complex multilayer high reflectivity coatings, the uniformity may be degraded somewhat within 1 – 2 mm of the edge of the coated area. The BFA étalon has a central element, which is optically contacted to the base plate. The MRF étalon, by contrast, has no central element (Figure 2).

The étalons have three drive and three reference capacitors, situated at 120 ° around their circumference (Fig. 2). The right hand side of the drawing shows the construction of the spacer elements, with two fused silica end caps and six Piezo-electric Transducer (PZT) elements. The drive capacitors are constructed of two cylindrical elements. One is optically

contacted to the top étalon plate and the other to the bottom. Since the two parts of the drive capacitor are connected to each étalon plate, the capacitor is able to act as a proxy, essentially measuring any changes in the étalon plate separation and hence the optical path difference or parallelism.

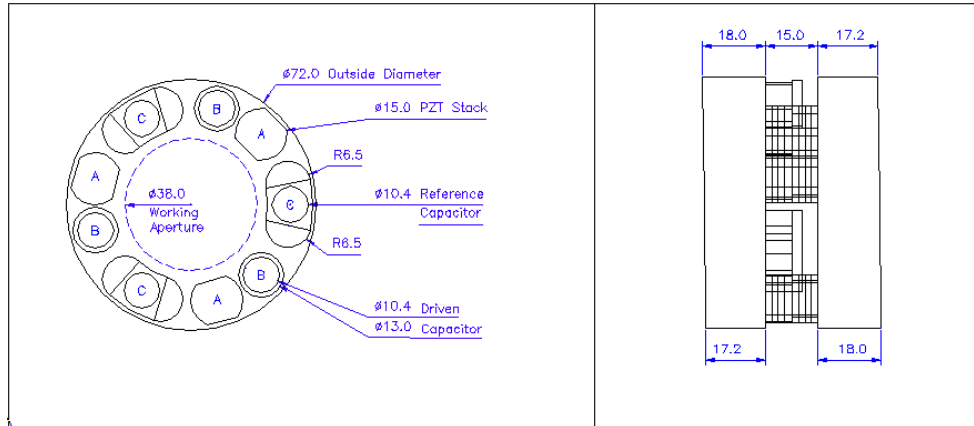


Fig. 2. Schematic diagram of the BFA étalon (all dimensions are in mm); A is the PZT stacks, B is the drive capacitors, and C is the reference capacitors.

3.2 The Mechanical Mounting structure

The mechanical structure or cage, used to hold and mount the completed étalon, is a critical component within ALFA. The cage performs several important tasks. It is essential for protecting the CSE from excessive mechanical loading during launch and it must also minimise the effects of any thermally-induced effects on the étalon.

The basic mechanical design of the CSE and cage originated during the preparations for the NASA Dynamics Explorer (DE) mission [5, 6]. Considerable design and development was undertaken to produce a mechanical structure that would hold the DE étalon in place through launch vibrations and thermal transients. This basic design of mechanical structure or cage has been further developed for use on successive CSEs [2].

The purpose of the mounting structure is as follows:

- To provide a secure mechanical constraint for the étalon with respect to environmental loads.
- To eliminate thermally induced loads on the étalon.
- To minimise thermal coupling between the cage mounting interface and the étalon.
- To minimise induced mechanical distortions on the étalon plate surfaces which might cause the étalon's optical performance to deteriorate.

A key design guideline applied to the revision of the mounting structure design was that the loads applied to the étalon plates by the cage structure must be such that the resulting forces are co-linear with the axes of the piezo-electric transducers. In this way, distortion of the étalon plates would be minimised.

A primary focus of the mechanical design activities for the ALFA project was to optimise the étalon support structure of the cage. The objective was to achieve a more efficient and robust design concept, minimising étalon plate distortion in operation, while providing adequate support to the étalon for the high vibrational loading of launch conditions. Finite Element (FE) analysis models were used to simulate the performance of traditional mounting structure [2,4,5]. The cage design was then optimised, minimising any induced distortions generated by the structure, while still ensuring that the étalon and cage would survive qualification level environmental testing.

A detailed description of the mechanical analysis is beyond the scope of this paper. An example of the analysis performed is shown in Fig. 3. The figure shows the stress levels in the cage structure expected during the vibration testing. Analysis of the information contained in Fig. 3 showed that the stresses in the cage and étalon plates were within the elastic limits of the respective materials throughout the envelope of the vibration and shock tests.

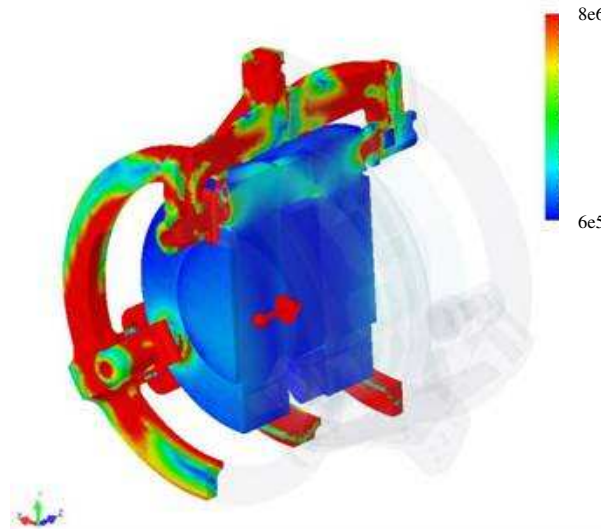


Fig. 3. An example of the finite element analysis performed in designing the CSE plate mounting structure.

The final cage structure, as manufactured, is shown in Fig. 4. The design shows that the mounting points are located directly over the PZT stacks. This ensures that any pre-load placed on the étalon results in minimal distortion of the étalon plates. The dimensions of the legs are optimised to fine-tune the resonant frequencies of the structure, thus ensuring that the étalon cannot be subjected to destructive forces during the vibration and shock testing programme required for space qualification.



Fig. 4. The complete mounting structure of the CSE.

As both CSEs are essentially air-spaced Fabry-Pérot étalons, they are sensitive to atmospheric pressure changes when tested in ambient (non-vacuum) conditions. In order to obtain the best optical performance the CSEs are, therefore, mounted within pressure sealed containers. Of course, these sealed containers are not required for testing or operation under hard space vacuum conditions. The ALFA filter assembly test bench is shown in Fig. 5.

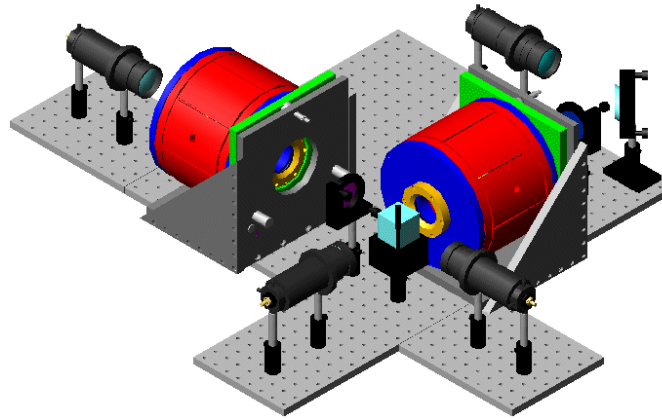


Fig. 5. The ALFA test bench.

Photographs of the completed and mounted BFA CSE are shown in Fig. 6. For programmatic reasons the BFA CSE was mounted in a second, un-blackened, structure for vibration testing (shown at the right of Fig. 6).

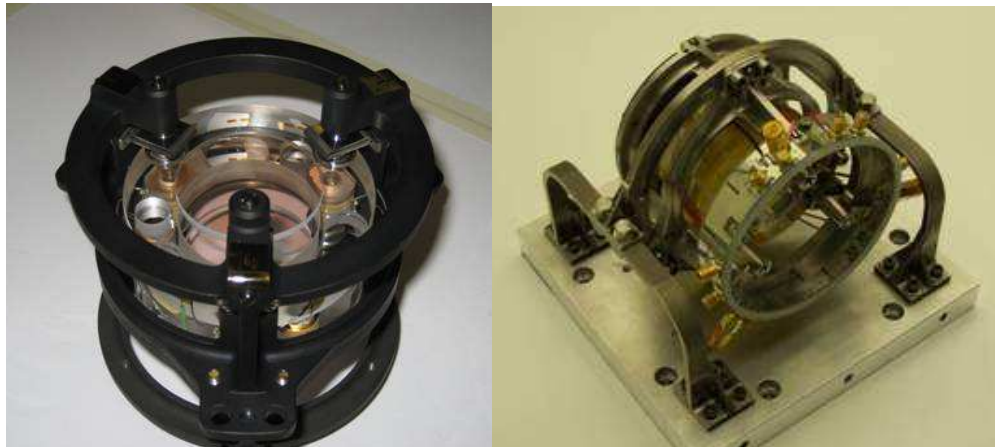


Fig. 6. The fully-assembled BFA étalon, mounted with its mechanical cage and structure.

Figure 7 shows the complete ALFA filter assembly as proposed for EarthCARE. The total mass of the complete filter is < 5 kg. In addition, a double-étalon electronic control unit is also required, the power consumption of which is < 15 W.

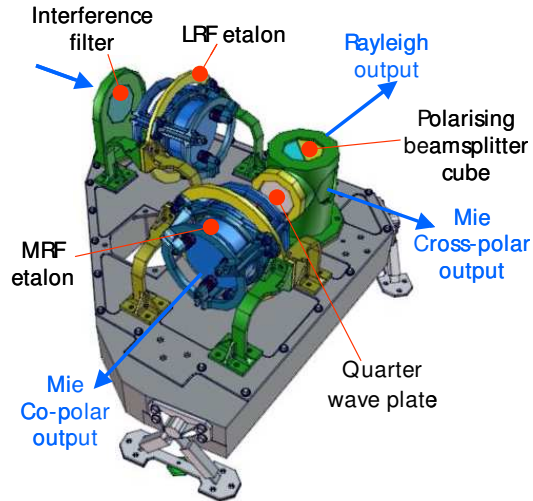


Fig. 7. The Space version of the ALFA assembly (design by Thales Alenia Space).

4. Testing

The primary test rig is shown in Fig. 8. The étalons were tested both individually and then in the complete ALFA assembly. The étalons were illuminated by a collimated beam of monochromatic light at 355 nm with a measured divergence 0.5 mrad, and a diameter of 38 mm at the input aperture of the first étalon. As shown in Fig. 8, a beam splitter was used to divert 4 % of the incoming light into a calibration channel. Four Thorlabs UV enhanced SM05PD7A PIN photodiode were used as the detectors, at the four points (10,11,12 and 13) shown in Fig. 8.

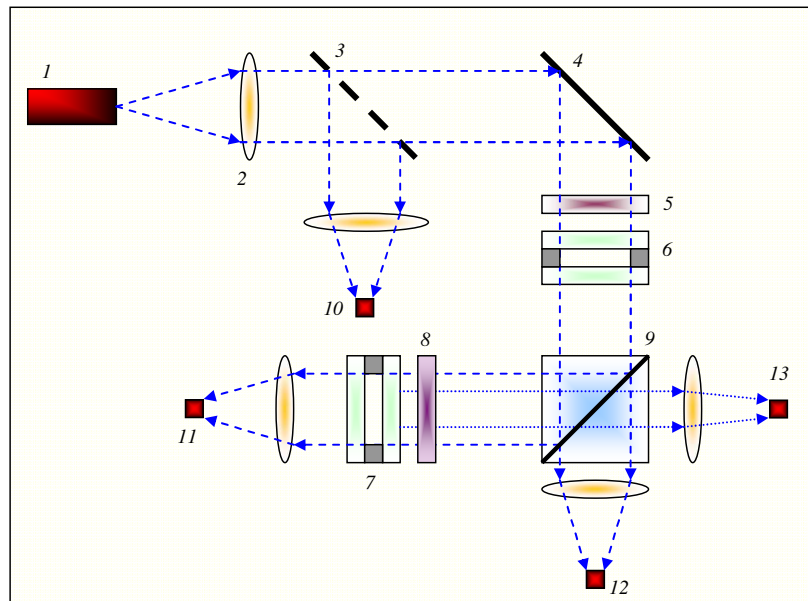


Fig. 8. The ALFA assembly test rig: 1: Laser source, 2: Lenses, 3: Calibration beam splitter, 4: Reflecting mirror, 5: Interference Filter, 6: BFA Fabry-Pérot étalon, 7: MRF Fabry-Pérot étalon, 8: $\frac{1}{4}$ Wave plate, 9: Polarising beam splitter, 10: calibration detection channel, 11: Mie Co Polar channel, 12: Mie Cross-polar channel, 13: Rayleigh Channel.

The illuminating source was a single frequency pseudo-CW 355 nm laser (Lumanova). The laser was tuneable over a 30 GHz range with a pulse to pulse jitter of < 1 MHz. The spectral bandwidth of the laser was < 65 MHz with a total output power of 15 mW.

To test the individual étalons, the Mie Cross-polar path was used with the BFA and MRF étalons interchanged as required. To build up the transmission profiles of the étalons, their OPDs were stepped in 300 pm increments. The transmission was then measured at each step throughout the entire wavelength tuning range available.

5. Results

5.1 CSE Performance

The measured transmission profiles of the BFA and MRF CSEs are shown in Fig. 9 and Fig. 10 respectively. In both cases, the transmission profiles were obtained by changing the étalon plate separation over their complete tuning range. The OPD of the BFA was scanned through two Free Spectral Ranges (FSR), whereas the MRF was scanned over one FSR. The transmission profiles were measured under ambient laboratory conditions

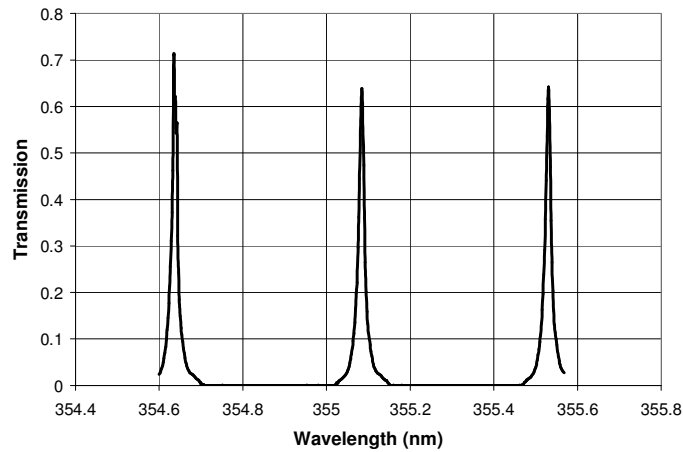


Fig. 9. The BFA CSE transmission profile.

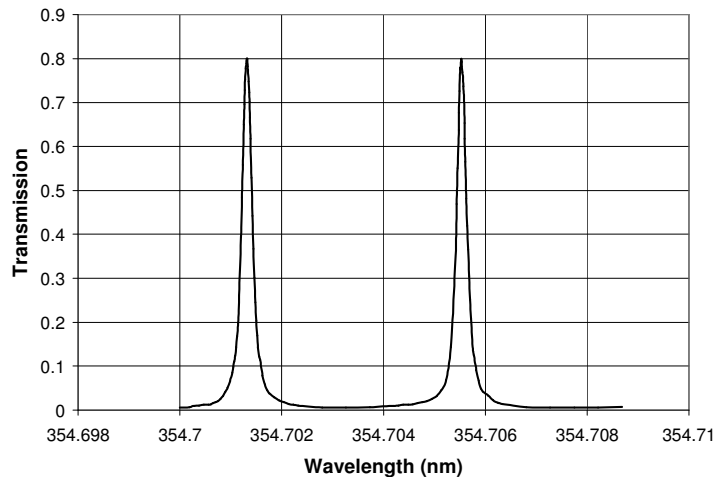


Fig. 10. The MRF CSE transmission profile.

These figures show that both étalons have excellent performance. The BFA demonstrates a finesse of 33 and a transmission of 70 %, while the MRF demonstrates a finesse of 22 with a transmission of ~ 80 %. In both cases the étalon can be tuned through at least one FSR. The slight apparent reduction in signal transmission observed in the BFA as the étalon is tuned is due to a time-dependent drift in the calibration channel. It should be noted that these tests do not directly measure the background rejection of the filters as they are illuminated by a monochromatic source.

Table 2 summarizes the measured performance of both the BFA and MRF CSE. The measured optical performance represents the current state of the art for filters of this size.

The measured values of the reflectivity of each of the étalons are 93.3 % and 89 % for the BFA and MRF étalons respectively. By combining the measured values of transmission and finesse it can be concluded that the plates of both of the Fabry-Pérot étalons must have a matching flatness of better than $\lambda/200$ (at 633 nm) over their working diameter.

Table 2. Measured performance of the BFA and MRF CSEs.

Etalon Parameter	Measured Values	
	BFA	MRF
FSR	0.45 nm	4.2 pm
FWHM	13.6 pm	0.19 pm
Finesse	33	22
Actuation range	> 4 FSR	> 4 FSR
Tuning resolution	0.97 pm	0.0094 pm
Peak Transmission	71 %	80 %

The transmission of the interference filter was measured to be 79 % with a FWHM of 0.8 nm and 355 nm.

5.2 The ALFA Performance

The performance of the complete ALFA was demonstrated by tuning the BFA CSE to its peak transmission position and stepping the MRF CSE across its full tuning range. The transmitted intensity was then measured at each of the output channels. The resulting profiles are shown in Fig. 11. With reference to Fig. 10, the filled circles represent the Mie Co-polar output, the red circles the Rayleigh component and the dashed lines the Mie cross-polar component.

Figure 11 provides a clear demonstration of the operation of the ALFA assembly. A slight (and progressive) reduction in the laser output is observed in each of the channels as the étalon is stepped throughout its range.

The Mie Cross-polar output is constant throughout the scan, as expected, whereas the Mie Co-polar and the Rayleigh channels are mirror-images of each other. As the transmission through the Mie cross-polar étalon increases so the output observed at the Rayleigh channel decreases. The performance of the individual filters is unchanged.

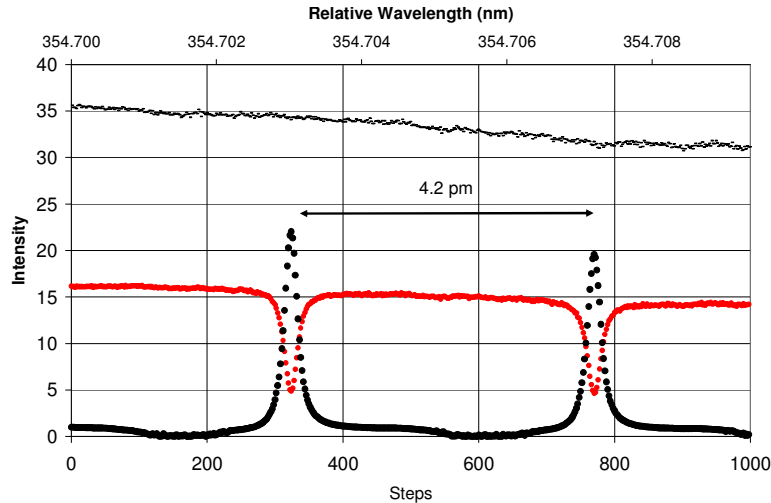


Fig. 11. Transmission profile of the ALFA assembly as a function of the MRF tuning position (steps of tuning): The filled black circles are the Mie co-polar output, red circles are the Rayleigh output, and the dashed lines are the Mie cross-polar output (units are μW).

The final measured optical performance of ALFA is compared with the programme requirements in Table 3.

Table 3. Measured performance of the BFA and MRF CSEs.

	Channel		
	Mie Cross-polar	Rayleigh	Mie Co-polar
Bandwidth	13.6 pm	13.6 pm	0.19 pm
Minimum target transmission value	55 %	50 %	45 %
Measured value	$56 \pm 1\%$	$51 \pm 1\%$	$46 \pm 1\%$

Additionally, the stability of the system was monitored over a 16 hour period. During this time the OPDs of both étalons were shown to drift by less than 200 pm.

5.3 Laser Tracking

One of the key characteristics of the CSE is its ability to allow the filter to track changes in the laser wavelength. This feature was tested during the development of ALFA. Figure 12 shows the results from one of the tests performed. The laser source has a spectral bandwidth of < 65 MHz. When this source is used to illuminate the ALFA, due to the narrow spectral FWHM of the étalon, the laser light will only be transmitted efficiently when the spectral transmission of the étalon overlaps perfectly with the wavelength of the laser source. With any spectral mis-adjustment, the transmitted signal will decrease rapidly. In this test, the power output of the laser was kept uniform and care was taken to ensure that the optical system was maintained in perfect alignment.

In Fig. 12, the black line represents the signal transmitted through the MRF. A simple predictive search algorithm was applied which adjusted the CSE OPD in order to maintain the transmitted signal at a level of approximately 1.3 (arbitrary units). The laser wavelength was then deliberately changed by a series of random small increments compared with the FWHM of the étalon's spectral bandwidth. Every time the transmitted signal (black line) decreased, the OPD of the CSE was driven (via the automatic predictive search algorithm) to compensate for the induced change of the laser wavelength, until the peak intensity was recovered.

The red line shows the corresponding changes of Optical Path Difference of the CSE. It can be seen that the transmitted signal recovers to the level of 1.3 (arbitrary units) within a maximum of two adjustments of the CSE OPD. For these tests, there was no a-priori knowledge of the direction or magnitude of the laser wavelength drift, thus explaining the occasional need for two adjustments, the first having being made in the “wrong” direction.

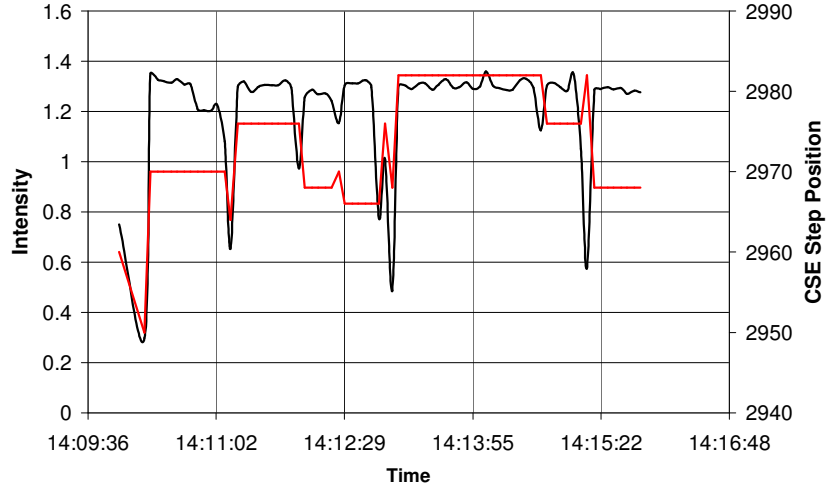


Fig. 12 . Tracking of the laser wavelength drift by the MRF CSE. The black line is the measured intensity; the red line is the CSE tuning position. (Intensity was measured in μW).

5.4. Environmental testing

Environmental testing was performed on the BFA CSE since this unit had the most exacting optical performance and construction. Environmental testing consisted of high sine, random vibration tests and thermal cycling under vacuum conditions. A structural model of the BFA CSE was also subjected to shock testing. The vibration levels to which the étalon was subjected are summarised in Table 4 and Table 5.

Table 4. High sine vibration levels.

Frequency range (Hz)	Qualification level acceleration
5 - 24.9	12 mm (amplitude)
24.9 - 100	30 g
100 - 150	3 g
<i>Sweep rate</i>	<i>2 octaves/min</i>

Table 5. Random vibration levels.

Frequency range (Hz)	Qualification levels
20 - 100	+ 3 dB/octave
100 - 125	0.3 g^2/Hz
125 - 135	Downslope
135 - 240	0.05 g^2/Hz
240 - 250	Upslope
250 - 400	0.3 g^2/Hz
400 - 2000	- 3 dB/octave
<i>Overall (g RMS)</i>	<i>16.3 g RMS</i>
<i>Duration</i>	<i>120 sec / axis</i>

A complete description of the entire vibration testing programme and the results from those tests are beyond the scope of this paper. Thus only a brief summary is presented here.

Figure 13 shows a typical response of the BFA CSE to the “low sine” vibration, the red line shows the predicted response while the measured response is indicated by the maroon trace. The peaks indicate resonant frequencies within the cage. It indicates the very good agreement between predicted and measured performance. Following the extensive sine surveys (which also included tests on a structural model and mass dummy), the BFA CSE was successfully tested to 16.3 g rms random vibration and 30 g, 100 Hz high sine. To the knowledge of the authors, these are the most challenging vibration levels to which a Fabry-Pérot étalon of this size has ever been subjected.

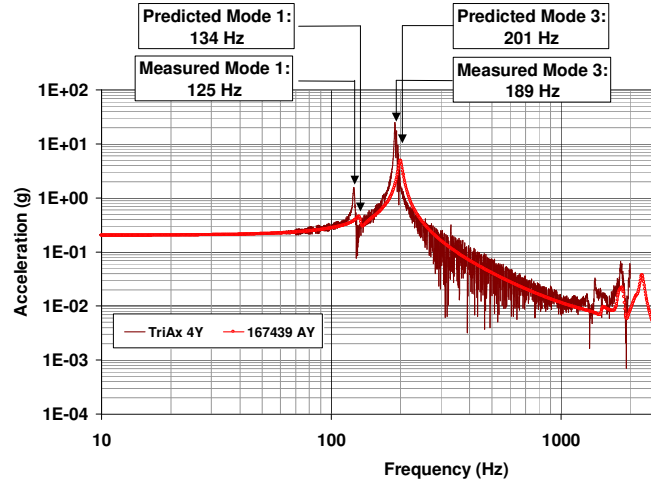


Fig. 13. Low-level sine response in the (y) axis.

Measurements of the optical properties of the BFA CSE were performed before and after the separate vibration and thermal vacuum tests. No significant changes were observed in the optical performance in critical comparisons of the tests made before or after any of the tests.

The étalon was also subjected to representative thermal-vacuum testing. This consisted of subjecting the equipment to four non-operational cycles between 0°C and 35°C. As was the case with the vibration tests, the étalon performance was measured before and after the test. No changes in the performance of the étalon were observed. The trace of the recorded temperatures at various points within the étalon and cage structure during the thermal vacuum tests is shown in Fig. 14.

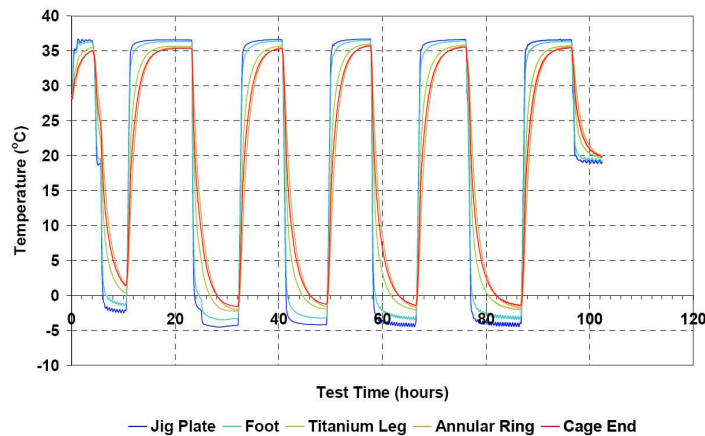


Fig. 14. Temperature profiles measured by temperature sensors during thermal-vacuum tests.

For correct operation in space, the effect of vibration on the complete ALFA system must be assessed. The alignment of the étalon and other equipment within the instrument must be maintained to an accuracy of 0.5 mrad. In addition, the ALFA system, as with any other complex optical instrument, must be tolerant to issues related to out-gassing and high energy radiation. These are well known problems. They are mitigated by selecting appropriate materials for the étalons, the coatings and other components within the instrument. It is also essential to apply carefully regulated processes for handling and storing the components and the instrument throughout the entire space development and fabrication programme.

6. Summary and conclusions

A new Mie / Rayleigh separation filter assembly (ALFA) has been developed as a candidate system for the ATLID LIDAR instrument for the EarthCARE Mission.

In optical terms, the filter performed excellently, meeting the demanding transmission requirements of the three primary detection channels (Mie co- and cross-polar and Rayleigh). Individually the critical components of the filter chain (the CSEs) have delivered performances that are state-of-the-art for étalons of such apertures at 355 nm. The étalons have demonstrated finesse values of 33 and 22 and transmission values of 71 % and 80 % respectively. ALFA has also shown an ability to track laser wavelength drift on < 100 ms time scales and with a demonstrated long-term stability in OPD of better than 200 pm.

The environmental testing of the CSE also met the programme objectives, leading to the successful engineering-level qualification of the mechanical design of the CSE, its cage and its mounting structure.

In conclusion, the ALFA development programme has shown that the CSE technology is well able to meet the requirements of Mie/Rayleigh separation. With the successful engineering – level space qualification of the mechanical aspects of the CSE, the technology is now ready for space flight application.

Acknowledgments

The authors would like to thank the European Space Agency for providing the financial support for this work.